Supporting Information to

Dramatically Enhancing Electrochemiluminescence Performance in Aqueous Phase Using Naphthalene Diimides with Excellent Electron-Transfer Capability and Water Solubility

Dalong Xu, Yuqi Wang, Mingxiu Tian, Liuxiang Chen, and Zhengang Han*

Key Laboratory of Water Environment Protection in Plateau Intersection (Ministry of Education), Key Laboratory of Bioelectrochemistry and Environmental Analysis of Gansu Province, College of Chemistry and Chemical Engineering, Northwest Normal University, Lanzhou 730070, China.

E-mail: hanzhengang@nwnu.edu.cn

Table of Contents

1. Chemicals and materials

In the experiment, all reagents were of analytical grade and purchased from Sinopharm Chemical Reagent Co., Ltd. (Shanghai, China). Reactions sensitive to oxygen or moisture were conducted under anhydrous and inert (N_2 or Ar) conditions. Nuclear magnetic resonance (^{1}H NMR) spectra were recorded on a Bruker Avance 400 MHz spectrometer using deuterated tetramethylsilane (Me_4Si) as an internal standard. Electrospray ionization mass spectrometry (ESI-MS) was performed using a Shimadzu LCMS-2010EV instrument. pH measurements were carried out using a Mettler Toledo SevenMulti pH meter (S40, Switzerland).

2. Preparation of NCD, NDI-N, and NDI-Cl

In this experiment, reactions sensitive to air or moisture were conducted in dry reaction tubes under argon protection. All organic solvents employed underwent rigorous dehydration and deoxygenation treatments. Analytical-grade reagents, including 1,8,4,5-naphthalenetetracarboxylic dianhydride, 3-dimethylaminopropylamine, 3-chloro-1-propanol, and methyl chloride, were purchased from Sinopharm Chemical Reagent Co., Ltd. (Shanghai). ^{1}H NMR spectra were acquired using a Bruker AV 400 M NMR spectrometer, with chemical shifts referenced to tetramethylsilane (TMS) in deuterated solvents. Electrospray ionization (ESI) mass spectra were recorded on a Shimadzu LCMS-2010EV mass spectrometer. The compounds dimethyl 2,7-bis[3-(dimethylamino)propyl]-1,8,4,5-naphthalenetetraformyl diimide and 2,7-bis[3-(trimethylamino)propyl]-1,8,4,5-naphthalenetetracarbodiimide are abbreviated as NDI-N and NDI-Cl, respectively (Scheme S1). These compounds were synthesized following a slightly modified protocol from the literature (Scheme S1)[S1].

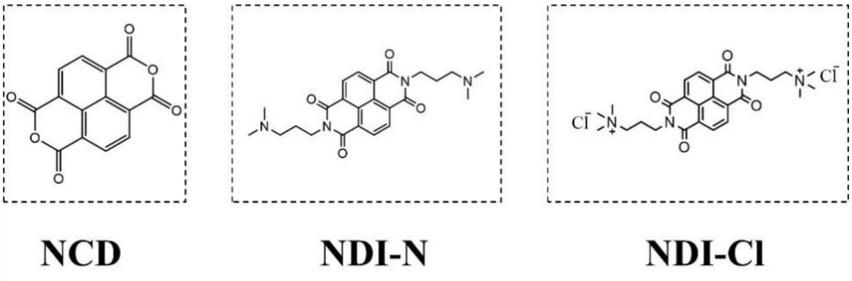

Scheme S1. Chemical Structures of NCD, NDI-N, and NDI-Cl

(1) **The compound NCD was obtained as a commercial reagent from Sinopharm Chemical Reagent Co., Ltd (Shanghai) as analytical purity. Its chemical structure was characterized by ^{1}H NMR and mass spectrometry (MS).**

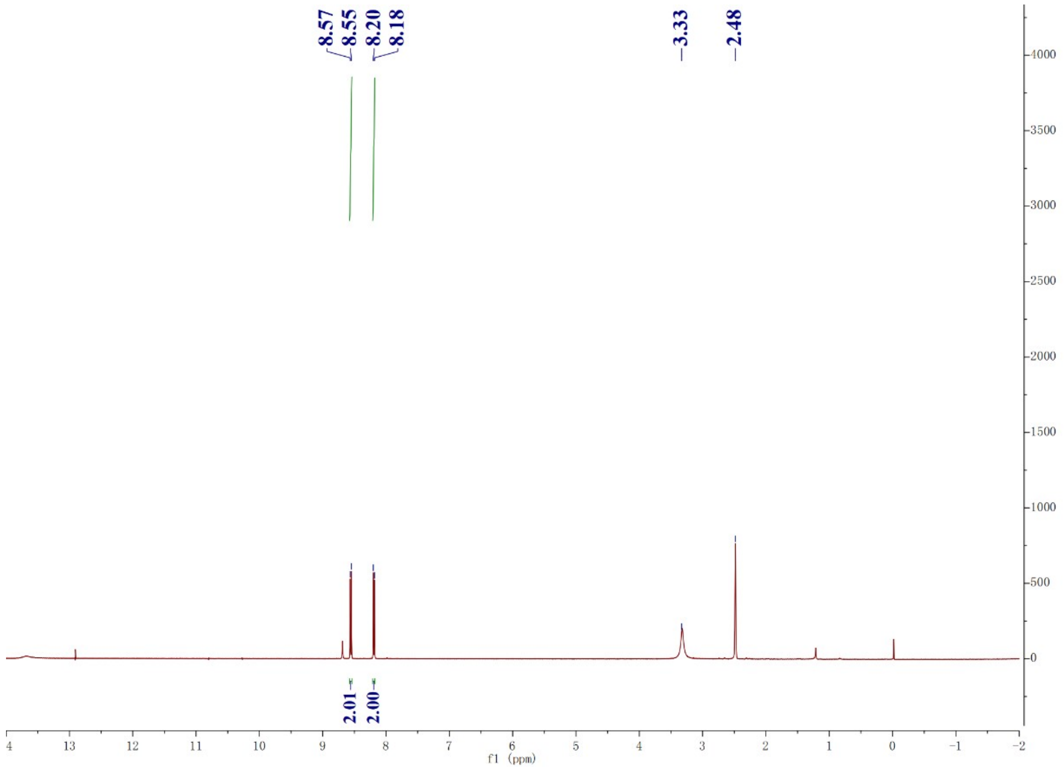

Figure S1. The ^{1}H NMR spectrum of NCD. ^{1}H NMR (400 MHz, DMSO-d_6): δ 8.57-8.55 (d, J = 7.5 Hz, 2H), 8.20-8.18 (d, J = 7.5 Hz, 2H).

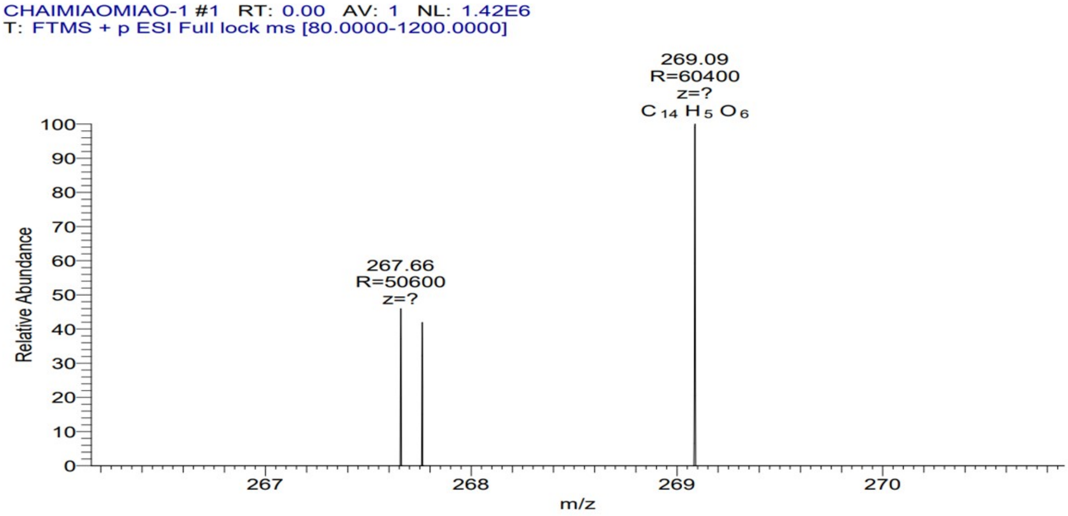

Figure S2. The mass spectrum (MS) of NCD. MS (ESI): m/z = 269.09(M+H).

(2) Sythesis of 2,7-Bis [3-(dimethylamino) propyl] -1,8,4,5-naphthalenetetraformyl

diimide (NDI-N).

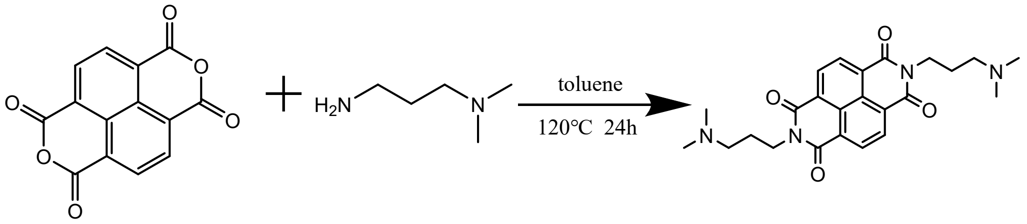

Scheme S2. Synthetic routes of NDI-N

In an autoclave reactor, 1,4,5,8-naphthalenetracarboxylic dianhydride (NTCDA) (15 g, 56.0 mmol) was combined with 3-dimethylaminopropylamine (17.15 g, 168 mmol) in 100 mL of toluene. Then transfer the solution to a stainless steel high-pressure sterilizer lined with 200 mL of polytetrafluoroethylene (PTFE) and heat it to 120 °C for 24 hours. After the reaction, filter the product, wash it three times with H_2O and ethanol, and dry it overnight in a vacuum drying oven to obtain yellow crystal NDI-N. Yield: 23.19 g (95%). ^{1}H NMR (400 MHz, $CDCl_3$) δ 8.74 (s, 4H), 4.29-4.22 (m, 4H), 2.44 (t, J=7.1 Hz, 4H), 2.23 (s, 12H), 1.96-1.87 (m, 4H).

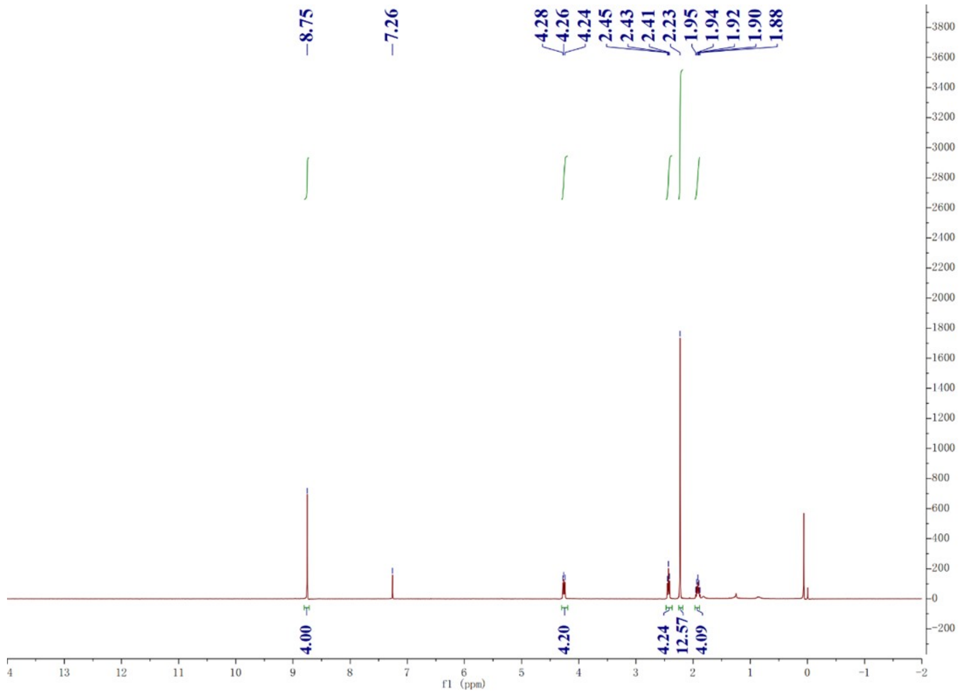

Figure S3. The ^{1}H NMR spectrum of NDI-N. ^{1}H-NMR (400 MHz, $CDCl_3$): δ 8.74 (s, 4H), 4.29-4.22 (m, 4H), 2.44 (t, J=7.1 Hz, 4H), 2.23 (s, 12H), 1.96-1.87 (m, 4H).

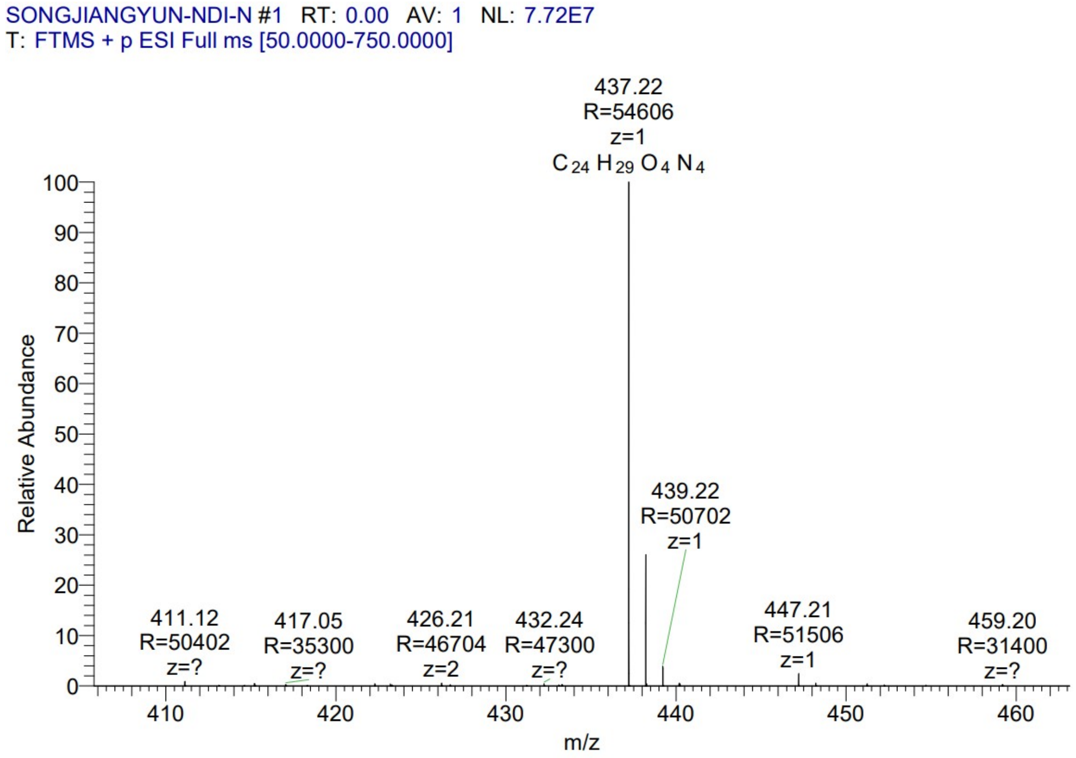

Figure S4. The mass spectrum (MS) of NDI-N. MS (ESI): m/z = 437.22(M+H).

(2) Sythesis of 2,7-Bis [3-(trimethylamino)propyl]-1,8,4,5-naphthalene tetracarbon diimide

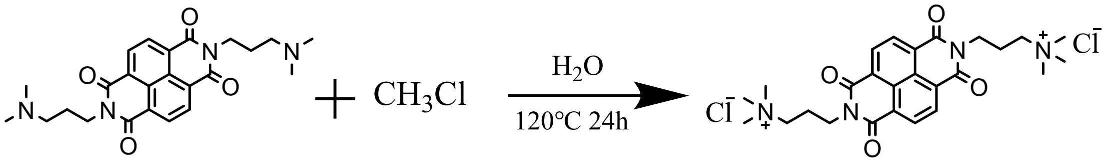

Scheme S3. Synthetic routes of NDI-Cl

In an autoclave reactor, NDI-N (15 g, 34.4 mmol) was combined with chloromethane (103.1 mL, 1.0 mol L-1 In tetrahydrofuran, THF, 103.1 mmol). Then transfer the solution to a stainless steel high-pressure sterilizer with a PTFE liner (200 mL) and heat it to 120 ° C for 24 hours. After the reaction, pure product precipitated. After filtration, washing with acetone three times, and vacuum drying, a gray white NDI powder was obtained. Yield: 17.7 g (96%). ^{1}H NMR (400 MHz, D_2O): δ 8.60 (s, 4H), 4.22 (t, J=6.9 Hz, 4H), 3.56-3.46 (m, 4H), 3.12 (s, 18H), 2.31-2.20 (m, 4H).

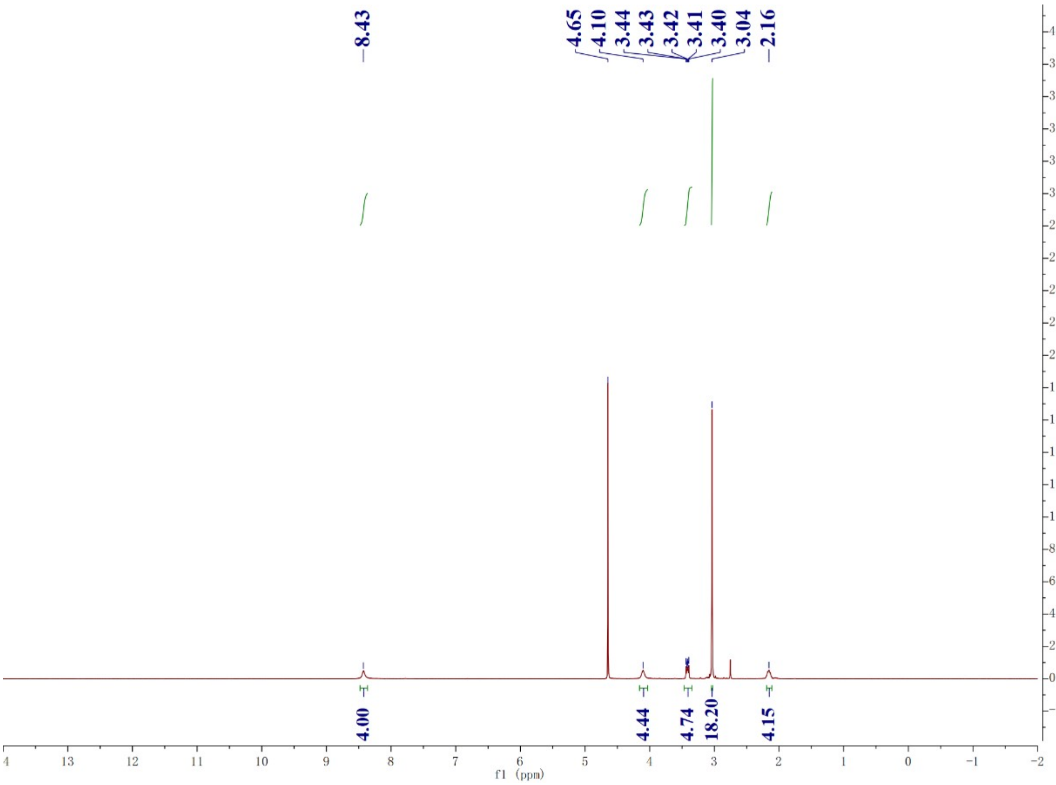

Figure S5. The ^{1}H NMR spectrum of NDI-Cl. ^{1}H-NMR (400 MHz, D_2O): δ 8.60 (s, 4H), 4.22 (t, J=6.9 Hz, 4H), 3.56-3.46 (m, 4H), 3.12 (s, 18H), 2.31-2.20 (m, 4H).

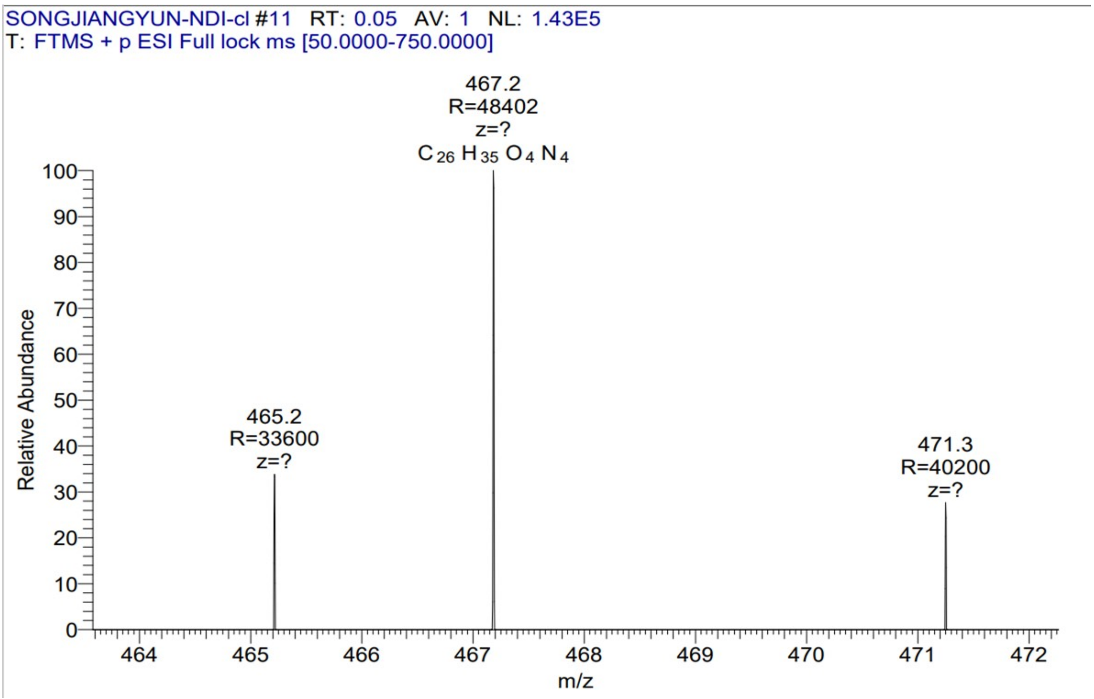

Figure S6. The mass spectrum (MS) of NDI-Cl. MS (ESI): m/z = 467.2(M+H).

3. Optimized molecular orbital plots of NDI derivatives

Density functional theory (DFT) calculations were carried out using the Gaussian 03 package (Rev. C.01). Geometry optimizations, molecular orbitals, and electronic structure analyses were performed at the B3LYP/6-311G(d,p) level.

4. Photophysical properties of NDI derivatives

UV-Vis absorption spectra were recorded on a UV-1102 spectrophotometer (Tianmei Scientific Instruments, Shanghai). Photoluminescence (PL) spectra were acquired using an Edinburgh FLS920 fluorescence spectrometer.

Table S1. UV-Vis absorption and luminescent data

Compounds	λ^{abs}_{max}(nm)	λ^{f}_{max}(nm)
NCD	348, 366	395
NDI-N	358, 378	403
NDI-Cl	362, 382	415

5. ECL measurements

Initially, a glassy carbon electrode (GCE, 3 mm in diameter) was polished to a mirror-like finish using alumina slurry (0.05~0.1 μm). Subsequently, the GCE was sonicated sequentially in deionized water, ethanol, and deionized water, thoroughly rinsed with ultrapure water, and dried under an infrared lamp in a nitrogen stream. Cyclic voltammetry (CV) was performed (potential range: −2.0 to 2.0 V; scan rate: 0.1 V/s) until a stable redox wave of $K_3[Fe(CN)_6]$ was obtained. The modified GCE was then prepared by drop-casting 5 μL of 10.0 mmol/L cyclopentadienol-based aggregates in THF/H_2O onto the surface of the cleaned GCE, followed by drying under an infrared lamp to form a dense film.

The redox properties of NCD, NDI-N, and NDI-Cl were characterized by CV, with relevant data acquired using an electrochemical workstation (CHI660E, Chenhua, Shanghai, China). For electrochemiluminescence (ECL) measurements, an MPI-A ECL detector (Remex, Xi’an, China) equipped with a custom-made 2 cm^3 electrolytic cell was used. ECL data were collected using a three-electrode system: a 3 mm diameter

GCE as the working electrode, a platinum wire as the counter electrode, and a saturated KCl Ag/AgCl electrode as the reference electrode. Prior to use, the working GCE was polished with alumina slurry, cleaned with ultrapure water, and dried under a nitrogen atmosphere. The photomultiplier tube voltage was set to 800 V for all electrochemical tests. ECL spectra were collected using a CHI 650D electrochemical workstation coupled with a fluorescence spectrophotometer (F97XP, Shanghai Cold Light Technology Co., Ltd.).

To prepare the measurement system, 0.5 μL of the luminophore solution (1.0 mM) was added to the custom-made electrolytic cell, followed by the addition of 0.1 M PBS containing 0.1 M KCl and 1.0 mM co-reactant $K_2S_2O_8$. The pH of the mixture was adjusted to 7.4, and the scan rate was set to 0.1 V/s. Finally, the corresponding electrochemical and ECL data were recorded using the MPI-A ECL detector. The ECL efficiency (Φ_{ecl}) was calculated by comparison with the standard tris(2,2'-bipyridine)ruthenium (II) ($Ru(bpy)_3^{2+}$)-based ECL system, using the formula:

$$\Phi_{ecl} = \Phi^{\circ}_{ecl} \times (I/Q) / (I^{\circ}/Q^{\circ})$$

Where: I and Q denote the integrated ECL intensity of the accumulated ECL spectra and the charge consumed (integrated from the voltammetric current vs. time curve) for the target system, respectively; Φ°_{ecl} represents the ECL efficiency of the standard $Ru(bpy)_3^{2+}$ system (1.0 mM $Ru(bpy)_3^{2+}$ in 0.1 M PBS [pH = 7.5] with 0.1 M $K_2S_2O_8$ as co-reactant), which was set to a relative value of 1; I° and Q° correspond to the integrated ECL intensity and consumed charge of the standard system, respectively.

Table S2. Calculated relative ECL efficiency systems

ECL Systems	**I**	**Q**	**Φ**
$Ru(bpy)_3^{2+}$	7580.5	0.2251	1
NCD	11143.2	0.2693	176%
NDI-N	15227.6	0.3125	278%
NDI-Cl	16667.3	0.3683	359%

6. Detection of ATP

ATP detection was performed by adding various concentrations of ATP (0, 20, 50, 100, 200, 500, 1000, 2000, 4000, 5000 μM) into the custom ECL cell containing 0.1 M PBS (pH = 7.5), 0.1 M KCl, and 1.0 mM $K_2S_2O_8$. The potential was scanned from 0.0 to −1.8 V (vs Ag/AgCl) at a rate of 0.1 V/s. The ECL intensity was recorded and plotted as a function of ATP concentration.

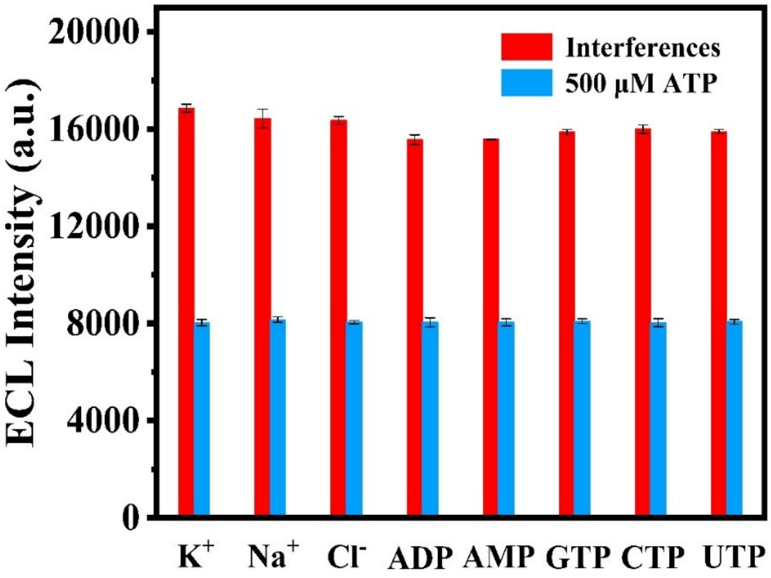

Figure S7. The quenching effect of various interferences in the ATP detection for the ECL system. The selectivity of the based ECL sensor was subsequently evaluated in the presence of potential interfering, including K^+, Na^+, Cl^-, adenosine diphosphate (ADP), adenosine monophosphate (AMP), guanosine triphosphate (GTP), cytidine triphosphate (CTP), and uridine triphosphate (UTP), within a solution containing 500 μM ATP.

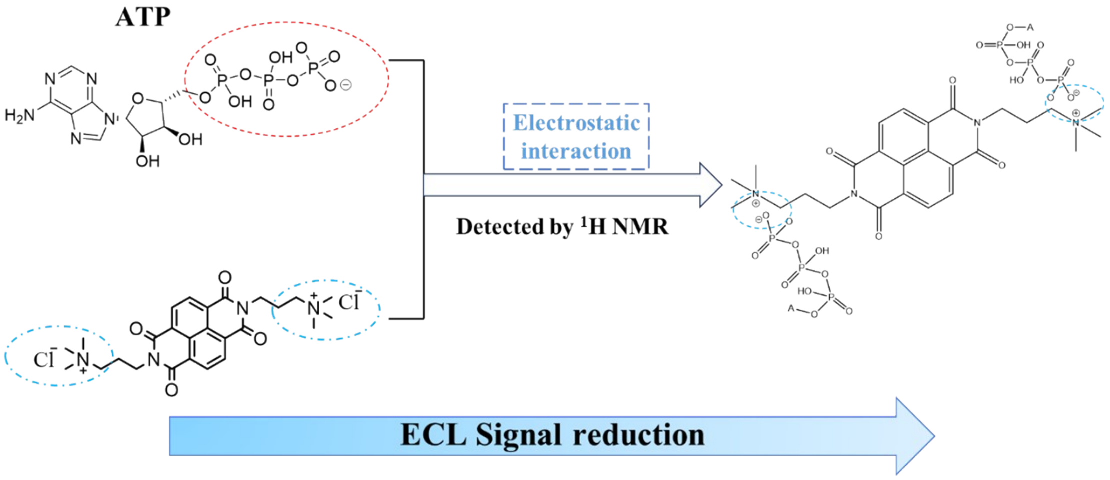

Figure S8. Schematic diagram of ECL analysis for ATP

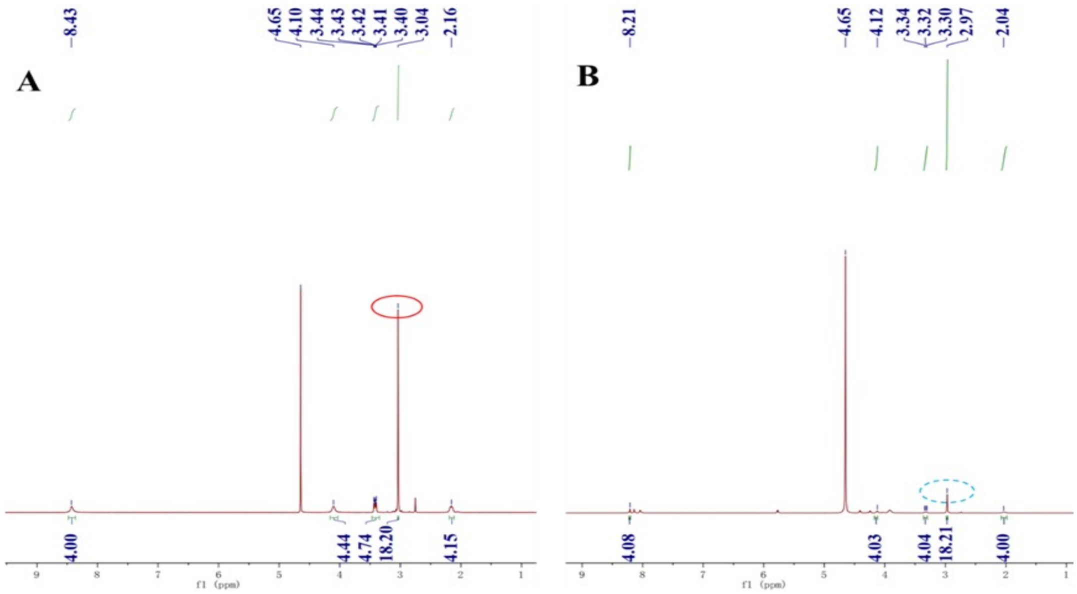

Figure S9. (A) The ^{1}H-NMR spectrum of NDI-Cl, (B) The ^{1}H-NMR spectrum of the mixture of ATP and NDI-Cl. The detection mechanism of ATP was investigated via ^{1}H NMR spectroscopy. Upon mixing ATP with NDI-Cl at room temperature, comparative analysis with the NMR spectrum of pristine NDI-Cl revealed distinct changes in the proton signal corresponding to the quaternary ammonium group (N^+-CH_3) of NDI-Cl: a significant reduction in peak intensity at 2.97 ppm and a slight upfield shift (from 3.04 ppm to 2.97 ppm), as highlighted in the red and blue boxes. These observations confirm the occurrence of electrostatic interactions between the triphosphate moiety of ATP and the quaternary ammonium groups of NDI-Cl, which in turn modulates the ECL signal of the system.

Table S3. Comparisons of the ATP analysis using different methods

Analysis methods	**Linear range**	**Limit of detection**	**Reference**
High-performance liquid chromatography	0.50~96.62 mg/kg	0.43mg/kg	S2
Circular dichroism	1.5~4.2 mM	0.2 mM	S3
Fluorescence (1)	0.5~15 mM	35 μM	S4
Fluorescence (2)	0.1~10 mM	0.033 mM	S5
Fluorescence (3)	0~3 mM	74.9 μM	S6

7. References

[S1] X. Liu, H. Zhang, C. Liu, Z. Wang, X. Zhang, H. Yu, G. He, *Angew. Chem. Int. Ed*., 2024, **63**, e202405427.

[S2] L. Zhou, X. Xue, J. Zhou, Y. Li, J. Zhao, L. Wu, *J. Agric. Food Chem*., 2012, **60**, 8994-8999.

[S3] P. Fu, M. Sun, L. Xu, X. Wu, L. Liu, H. Kuang, C. Xu, *Nanoscale*., 2016, **8**, 15008-15015.

[S4] Z. Wu, M. Liu, Z. Liu, Y. Tian, *J. Am. Chem. Soc*., 2020, **142**, 7532-7541.

[S5] K. Y. Tan, C. Y. Li, Y. F. Li, J. Fei, B. Yang, Y. J. Fu, F. Li, *Anal. Chem*., 2017, **89**, 1749-1756.

[S6] X. Zhou, S. Huang, D. Zhang W. Liu, W. Gao, Y. Xue, L. Shang, *Anal. Chem*., 2023, **95**, 12104-12112.